Technical Progress Report

Annual Report

Reporting Period: April 1, 2003 – March 31, 2004

Dr. Paul D. Ronney, Principal investigator

Report issued August 26, 2004

DOE Award # DE-FC26-02NT41336

University of Southern California
Department of Aerospace and Mechanical Engineering
Olin Hall of Engineering 430
Los Angeles, CA 90089

Disclaimer

Abstract

An ignition source was constructed that is capable of producing a pulsed corona discharge for the purpose of igniting mixtures in a test chamber. The corona generator can also be used as the ignition source for one cylinder on a test engine. The first tests were performed in a cylindrical shaped chamber to study the characteristics of the corona and analyze various electrode geometries. Next a test chamber was constructed that closely represented the dimensions of the combustion chamber of the test engine at USC. Combustion tests were performed in this chamber and various electrode diameters and geometries were tested. Higher peak pressures and faster pressure rise times were realized consistently in all test chambers versus standard spark plug ignition.

A test engine was purchased for the project that has two spark plug ports per cylinder to The data acquisition and control system hardware for the USC engine lab was updated with new equipment. New software was also developed to perform the engine control and data acquisition functions including cylinder pressure monitoring. A ceramic corona electrode has been designed that fits in the new test engine and is capable of withstanding the pressures and temperatures encountered inside the combustion chamber. The corona ignition system was tested on the engine and an increase in both peak pressure and IMEP were seen in the initial test. There are issues that must be addressed before on-engine testing can continue such as EMF interference from the corona generator and electrical insulation on portions of the piston and cylinder head to prevent arcing. The EMF issue can be solved with proper shielding and grounding and various ceramic coatings are being researched for electrical insulation.

Table of Contents

Experimental Apparatus

A. Corona Generator

The experimental set up consists of an electronic system to generate pulsed corona discharges and a combustion cylinder with measurement and gas handling system (Fig. 1). The pulsed power includes a high voltage pulse generator utilizing a thyratron (Triton F-211) and a Blumlein transmission line to create a high voltage pulse (typ. 30-55 kV) with narrow pulse width (typ. 150 nsec). The repetition rate was 1Hz and maximum pulse energy employed was 1.8 J. All the signals were displayed and recorded by a digital oscilloscope (Tektronix TDS 420A).

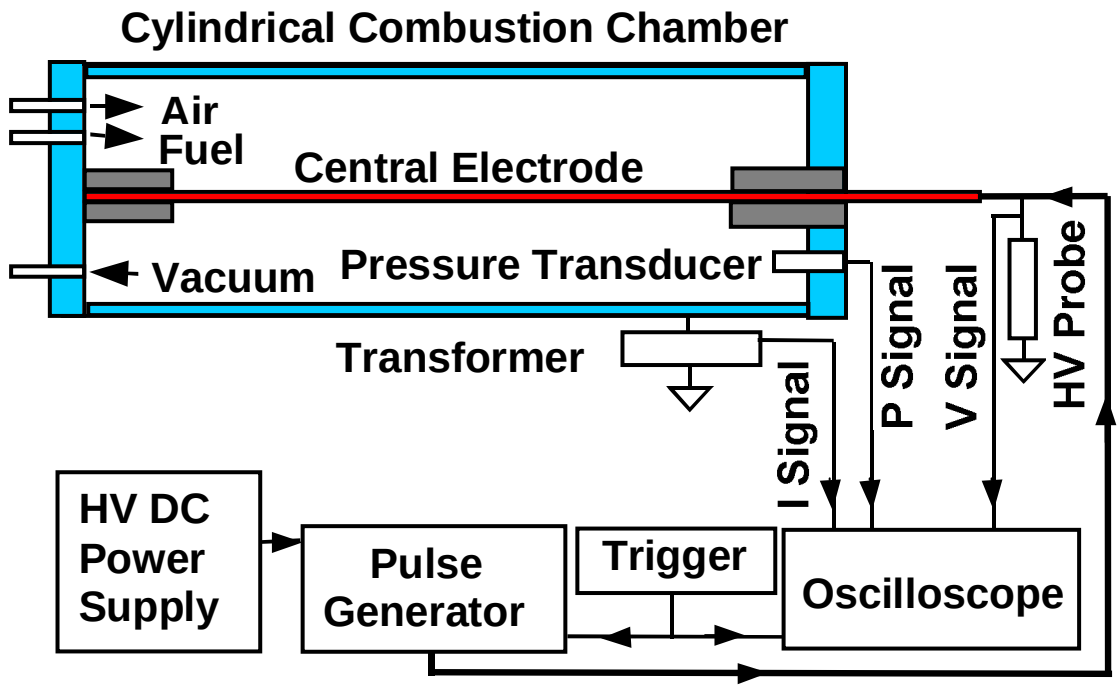

Figure 1. Experiment setup for investigation of flame ignition by pulsed corona discharge

The same equipment is used when running the corona on the engine. The firing is triggered from the optical encoder on the engine.

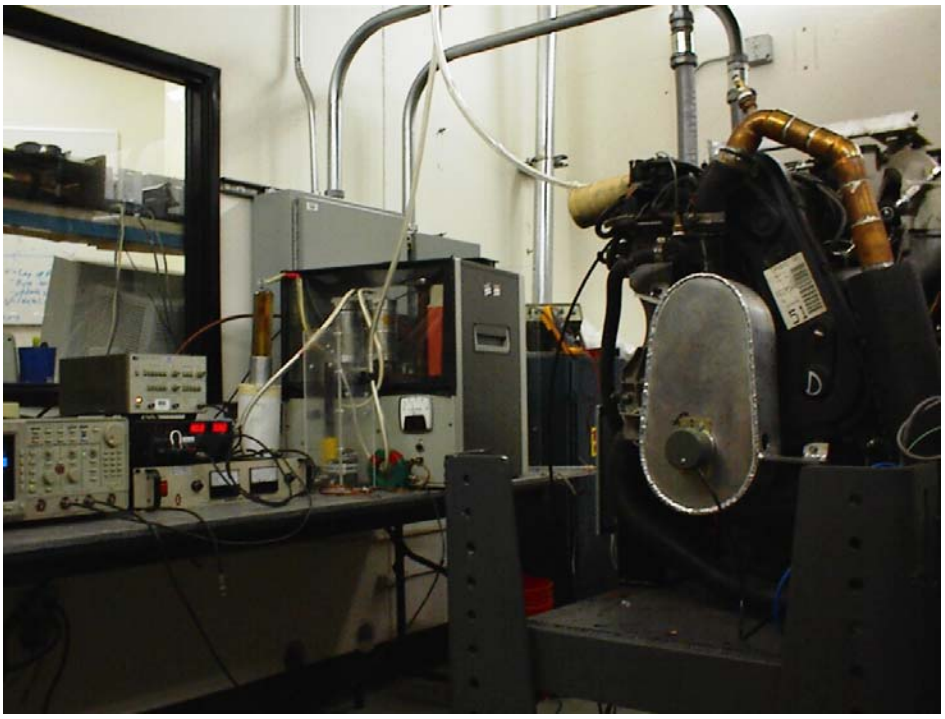

Figure 2. Corona generator connected to one cylinder on test engine

B. Test Chambers

Three different test chambers have been developed for testing of the corona discharge ignition. The first test cylinder is constructed from a 2.5" ID stainless steel tube that acts as the ground electrode. This chamber has an interchangeable metal rod placed at its central axis acting as the (central) electrode. The outer electrode is always grounded and the central electrode is connected to high voltage. In this report all reported experiments were done with positive corona (central electrode is anode) unless otherwise noted. There are gas inlets, outlet and vacuum pump inlet in one end plate and pressure gauge (Omega, DPG1000B), pressure transducer (Omega PX4201) and conventional car sparkplug (Bosch, platinum) on the other end plate. The sparkplug was switched by a standard car ignition circuit (GM Chevy Citation 81). A transparent plastic end plate was used for end view photos. This chamber also has a configuration that allows for testing under turbulent conditions (See Fig. 3).

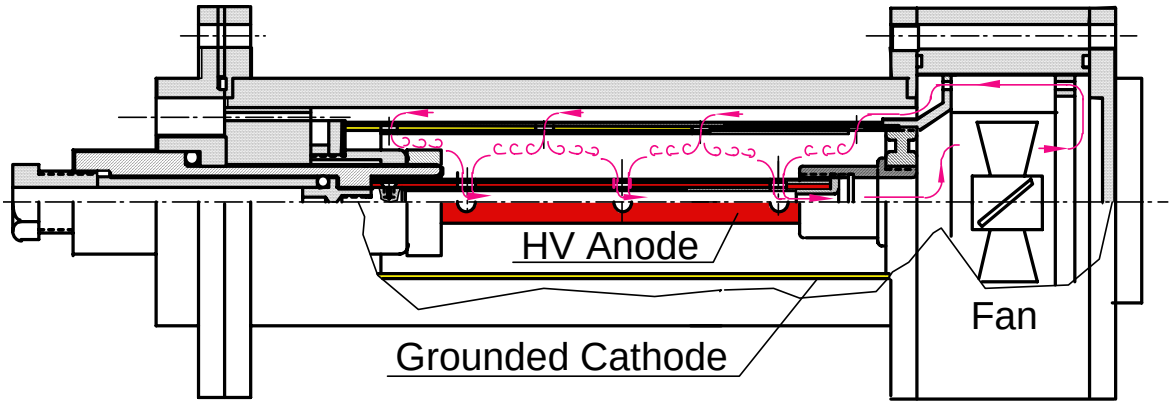

Figure 3. Cutaway diagram of turbulent test chamber with turbulence intensity of 0.5 to 1 m/s

The second test chamber used for the corona ignition experiments was modeled after the dimensions of the combustion chamber in the test engine. This chamber was constructed from 6061 T6 aluminum and consists of a bottom half that is machined into the shape of the piston dome of the test engine, and a top half that is machined to closely match the volume of the cylinder head. The two pieces are bolted together with six 5/16" bolts and are sealed with an O-ring (seen in Figs. 6 and 7). With this test chamber various electrode shapes and configurations could be tested much more quickly than in the engine. For tests performed at 1 atmosphere, the corona generator and the measurement equipment are identical to those used with the cylindrical shaped chamber. For tests run at elevated pressures a Kistler model 603B1 spark plug-mounted pressure transducer and model 5004 dual mode amplifier were used to measure the pressure. When performing ignition tests in this chamber the gas and air mixture was premixed in a larger chamber (Fig. 4). Combustion tests were performed at initial pressures up to 9.5 atmospheres. An alternate chamber top plate was fabricated from a ¼" plate of aluminum that leaves the sides open for photographing the test chamber (Fig. 7).

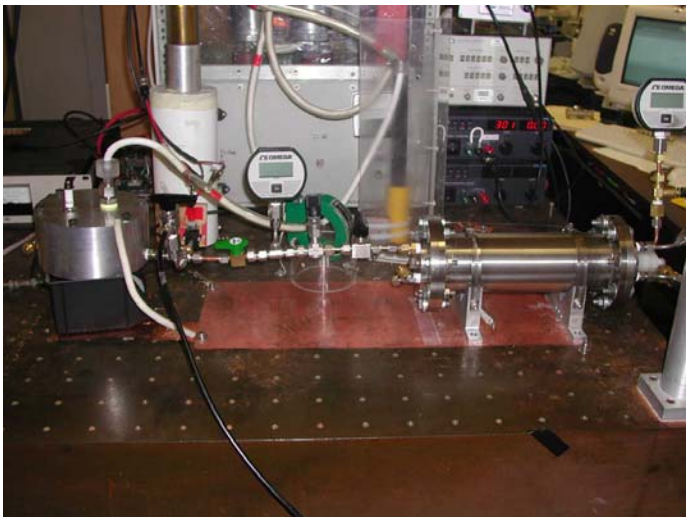

Figure 4. Experimental setup for engine cylinder test chamber

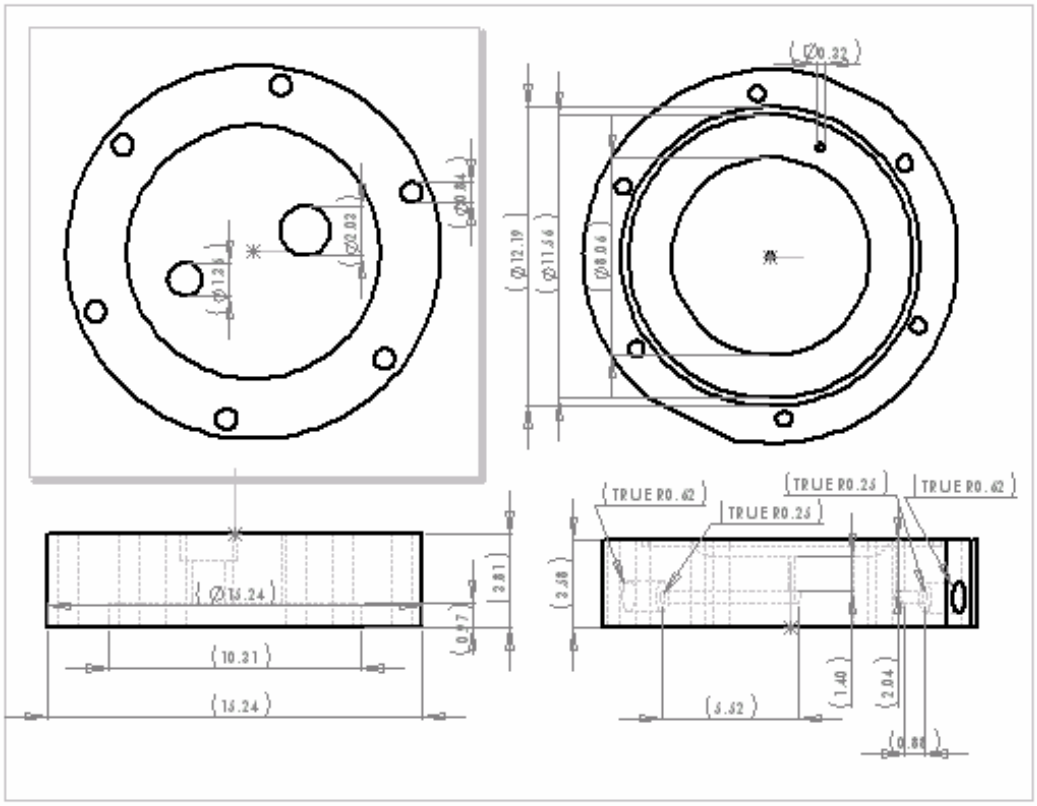

Figure 5. Dimensioned drawing of Engine Cylinder Test Chamber

Figure 6. Exploded view of Engine Cylinder Test chamber assembly, shown with circular ring electrode

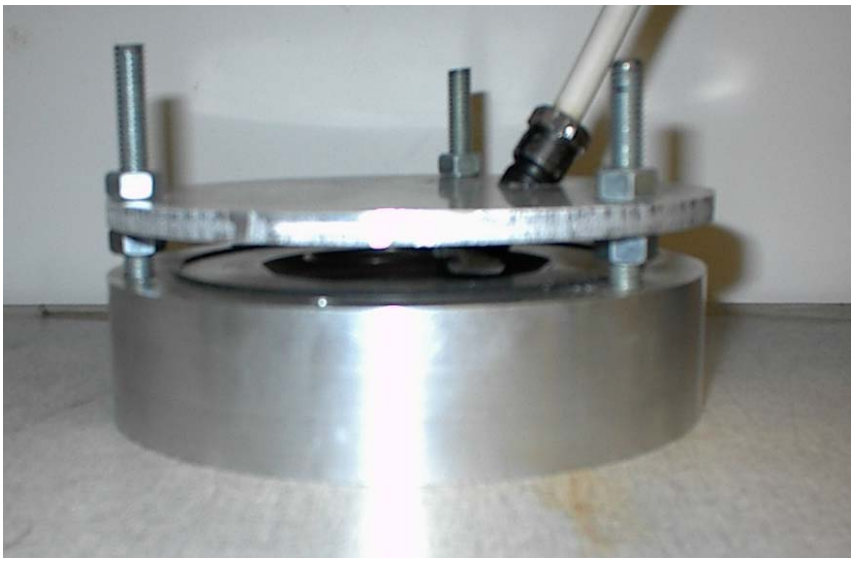

Figure 7. Engine cylinder test chamber in open configuration for visualizing corona discharge.

The third test chamber used in testing is constructed using a cylinder head and piston from the test engine described in below in section C. An aluminum block was machined to accept the piston from the test engine and holds the piston in a TDC position (see Fig. 9). The block has four holes that are tapped to accept the head bolts that secure the piston/block assembly to the head. The seal between the head and the block is held by using a head gasket from the engine. Gas handling is done through fittings installed in block-off plates that are installed over the intake and exhaust ports. Measurements are done with the same equipment used on the other test chambers. This chamber allows electrodes to be tested in a chamber with the exact same dimensions of the engine.

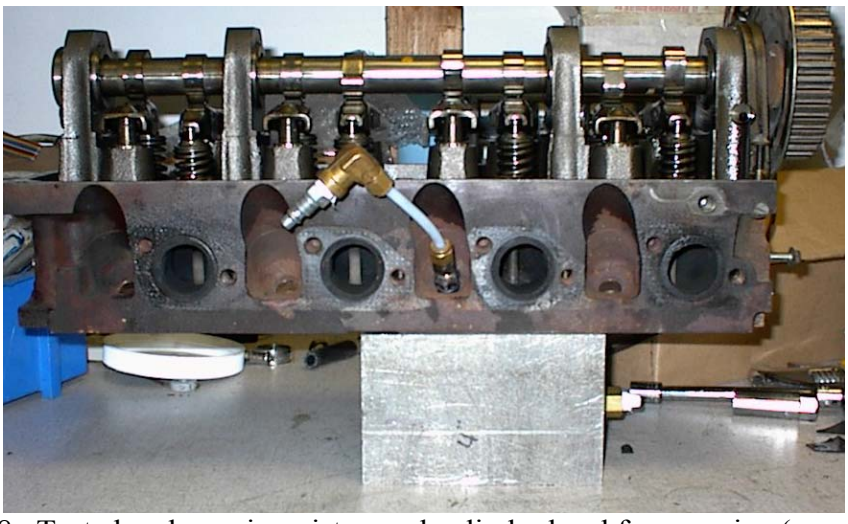

Figure 8. Test chamber using piston and cylinder head from engine (assembled).

Figure 9. Test chamber using piston and cylinder head from engine (disassembled).

C: Dual Plug Test Engine and Instrumentation

A new test engine as seen in Figure 10 was required to simplify the testing of the corona discharge ignition system in the engine. The engine purchased was a 2.5 liter 4 cylinder engine from a 2000 Ford Ranger Pickup. This engine was chosen because it has two spark plug ports per cylinder. This allows the corona electrode to be inserted into one of the ports and a conventional spark plug with cylinder pressure transducer to be inserted in the other. The engine was adapted to run on natural gas using the control valve and flow meter from the previous test engine.

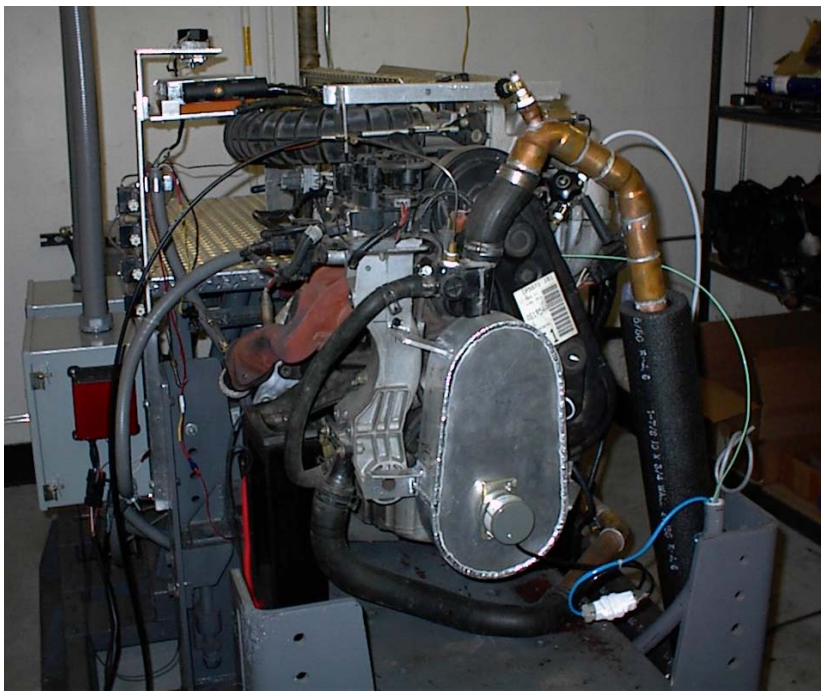

Figure 10. Test engine mounted to dynamometer.

New data acquisition and control hardware was purchased from National Instruments for the engine lab. This was necessary as the existing data acquisition equipment was obsolete and not compatible with a modern PCI bus PC. The new equipment consists of a PCI-6031E DAQ card, a PCI-7344 motion control card, an AMUX-64T terminal block for thermocouple inputs, a SCB-68 terminal block for analog inputs, a MID-7604 stepper motor driver and a CB68-LPR terminal block for digital IO (Fig. 11). The engine is fully instrumented and all critical pressures, temperatures and other parameters are monitored.

Figure 11. Main panel for data acquisition and control equipment. Top left AMUX-64T, top right SCB-68, bottom left MID-7604, bottom right CB68-LPR

New software was developed using LabView to interface with the new hardware. The software displays all of the pertinent engine parameters and incorporates PID control for the air/fuel ratio and dyno load control. The user interface was developed to be easy to read and user friendly (Fig. 12). Warning alarms and safety shutdowns were incorporated to protect the engine when parameters (pressures, temperatures or speed) get out of a safe range.

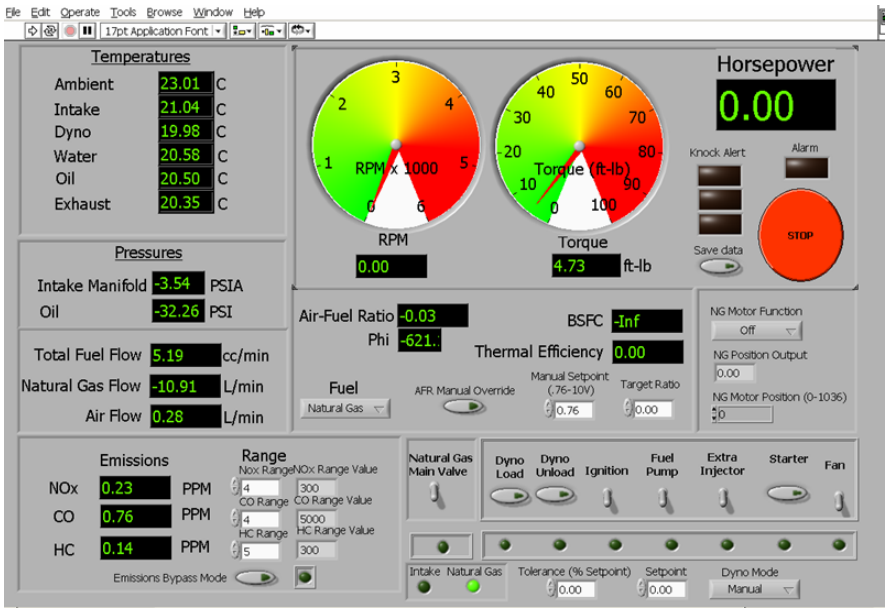

Figure 12. Screen capture of PC engine Control Panel

D. Cylinder Pressure Monitoring System

In order to quantify the performance characteristics of the corona discharge ignition system it was necessary to monitor the pressure of the cylinder that the corona electrode is installed in. A cylinder pressure monitoring system was designed to accomplish this task. The system consists of a Kistler pressure transducer with amplifier, an optical encoder coupled to the crankshaft with 2048 pulses per revolution (providing 0.18 degree resolution), and a high speed data acquisition card from National Instruments (NI 6070E). The amplifier was located in a shielded enclosure as was the terminal block for the wiring connections (Fig. 13).


Figure 13. Control cabinet for cylinder pressure monitoring system

The pressure transducer reads the cylinder pressure through a spark plug that was modified by Kistler with an added port for the transducer as seen below in Fig 14.

Figure 14. Modified spark plug with pressure transducer installed.

A program was created in LabView that collects cylinder pressure traces based on the trigger inputs received from the encoder that is mounted on the crankshaft. Cylinder pressure data is logged vs crank angle. This data is then imported into a spreadsheet where IMEP is calculated and PV diagrams are created (see Fig. 15.).

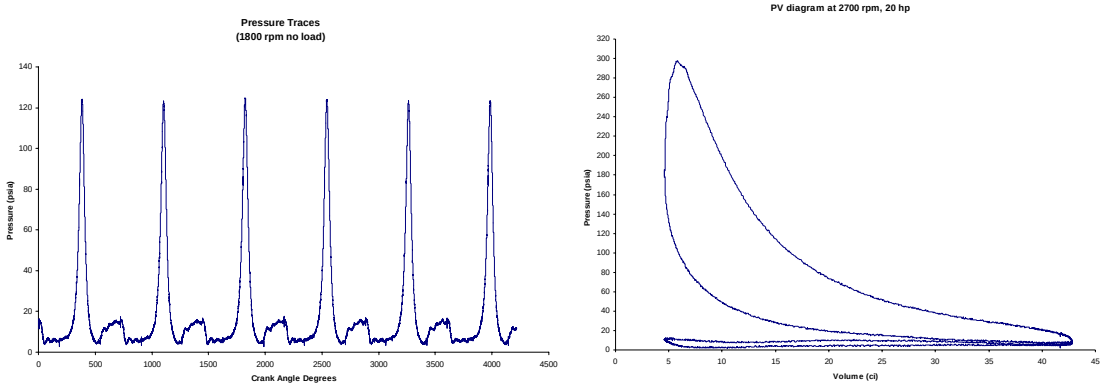

Figure 15. Examples of pressure data collected from engine (left) and pressure vs. volume diagrams that can be created from the data (right).

E. Ceramic Corona Electrode

The electrodes that were used for testing the corona in the test chambers were constructed of a plastic that could withstand the pressures of single shot combustion tests but not the temperatures encountered in a running engine. It was necessary to design an electrode that could withstand the temperatures and pressures of a running engine. A conventional spark plug could not be used as the conductor for the corona electrode as the electrical resistance is much too high for this application. The resistance should be as low as possible for the corona electrode to perform properly.

A machinable ceramic called Macor was chosen that has both high temperature resistance, good electrical insulating properties and is easily machinable. The steel body of the corona electrode uses a spark plug body with the original ceramic portion removed. The swaged lip was machined off the body that holds the ceramic in place. The Macor is purchased in ½" diameter rods and machined down to fit the steel spark plug casing. A shoulder is machined into the top of the ceramic rod which is captured by a steel ring installed from the top which is then welded to the spark plug body. A 1/8" brass rod is drilled from both ends to accept the electrode tip and the conductor. The brass rod is installed from the bottom and is held in place with a high temperature epoxy. This design allows different electrode tips to be used with one electrode body. The electrodes are hydro-tested at 1000 psi before they are placed into service in an engine.

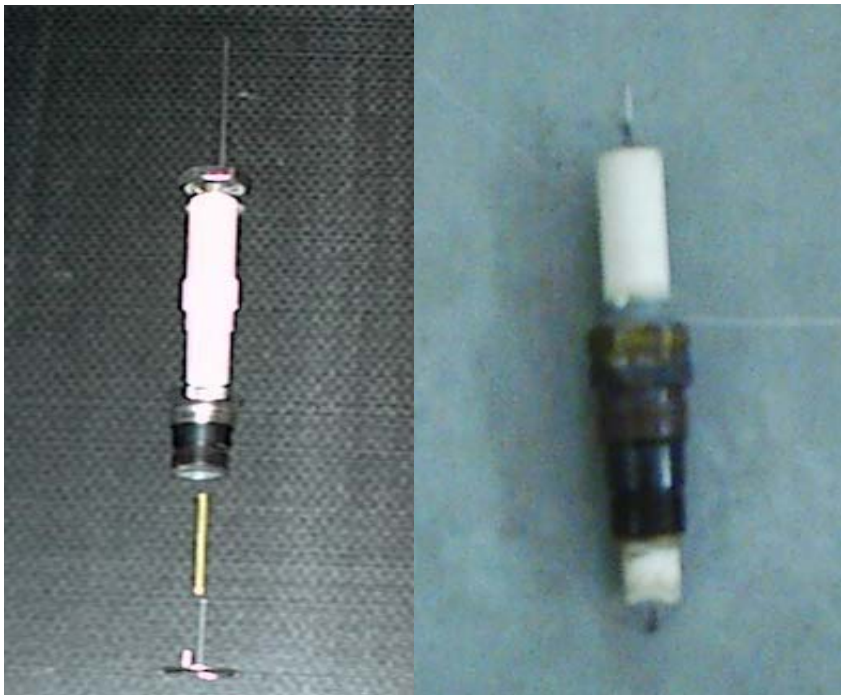

Figure 16. Ceramic corona electrode for running in engine show in exploded view (left) and assembled (right).

Results and Discussion

The experimental procedure for bench testing the corona discharge in the test chambers were as follows. Evacuate the test cylinder with a vacuum pump until the pressure gauge of 1/100 psi precision shows zero reading. Then fuel (CP grade) and air (dry cylinder air) were filled into the cylinder. Composition was controlled with a digital pressure gauge with precision of 1/100 psi. After igniting with either pulsed corona or spark discharge, pressure curve was measured by the pressure transducer. Pressure signals were read and recorded by the digital oscilloscope.

A. Electrical Characteristics

Photographs of various pulsed corona discharge are shown in Figs. 17 and 18. They were taken in a completely dark environment. Fig. 17 is a pulsed corona discharge with a plain electrode viewing from the end of cylindrical chamber. This shows many streamers distributed along the length of central electrode and superimposed with each other. If viewed from side many discrete streamers evenly distributed on the surface of the central electrode are evident. The average separation between streamers is 5mm and average diameter is 0.7mm. An estimated number of streamers on the central electrode is 600. When pulse energy was reduced from 356mJ/pulse to 44mJ/pulse the total number of streamers did not change noticeably, but the brightness of streamers decreased. Figure 18 shows the corona discharge from the side view in the open top chamber as seen in Fig. 7.

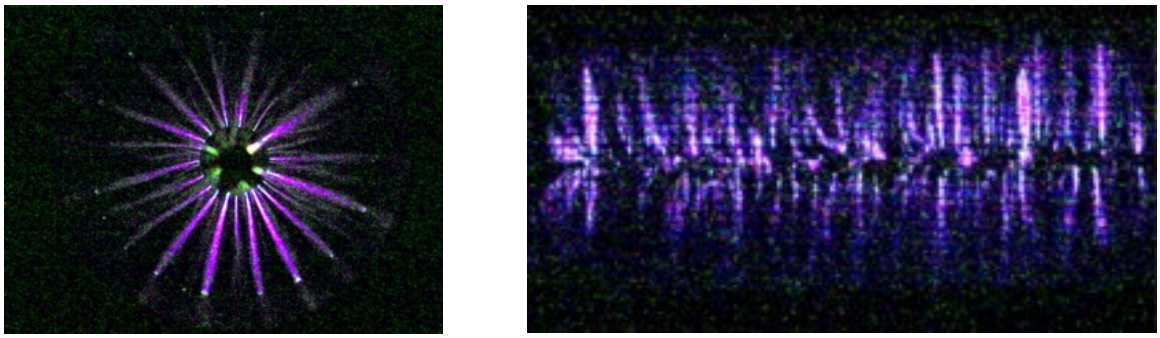

Figure 17. Left: Picture of pulsed corona discharge (end view). Diameter of central electrode: 6.35mm, Energy: 251mJ/pulse. Right: Picture of pulsed corona discharge (Side view). Diameter of central electrode: 6.35mm , Energy: 356mJ/pulse

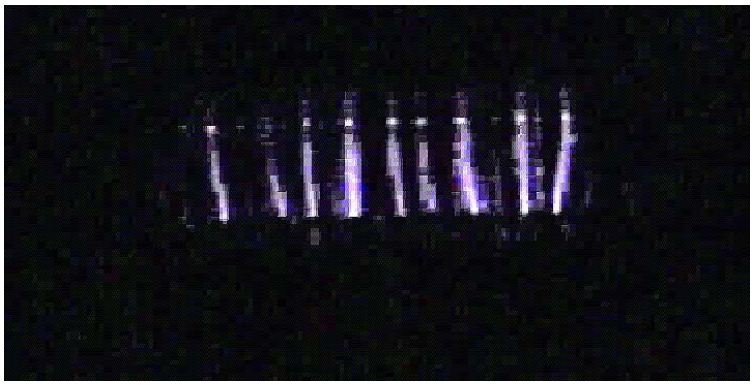

Figure 18. Photograph of corona discharge in engine cylinder test chamber with open top plate installed. .5mm diameter electrode 50mm circular ring

Figure 19 shows typical voltage, current and energy waveforms of pulsed corona discharges with (dashed curves) and without (solid curves) arcing. Current waveforms in Fig. 19b clearly show the difference between corona discharges with arcing and without arcing. Both dashed and solid curves have a first peak that corresponds to the corona discharge. Only the dash curve has the second current peak which correspondences to arc discharge. Comparing Figs. 19 a, b and c, one can see that after arcing (at 150ns after trig where current started to rise rapidly) voltage drops rapidly. Consequently, no rapid energy increase was observed on energy waveform (Fig. 19c) implying that arcing does not contribute significantly to energy input to plasma at the voltages at which arc is going to start, during times ≈100's nsec. In these experiments the experimental conditions (mainly the applied voltage and electrode structure) were so controlled that no arcs were observed to ensure that only the transient phase occurred before the formation of arcing. Typical voltage pulse width (FWHM) is 140ns, and current pulse width 80ns. Figures 20 and 21 show similar results for the engine cylinder test chamber.

Pulse energy as a function of peak voltage was observed for various electrodes. The pulse energy increases non-linearly and is faster at higher peak voltages. There is an intercept peak voltage, below which no energy output to plasma, i.e. pulse corona discharge starts at a certain value of peak voltage. The intercept peak voltage decreases as decreasing of diameter of central electrode. At the same peak voltage, a thinner central electrode provides higher pulse energy than a thick central electrode does. A threaded electrode produces higher pulse energy than smooth electrode (plain electrode) with the same diameter and peak voltage. In our particular conditions, brush-like electrodes provide best electrical performance. Positive corona discharge (central electrode is anode) is much better than negative corona discharge (central electrode is cathode). In the experiments reported below, only positive pulsed corona discharge is used.

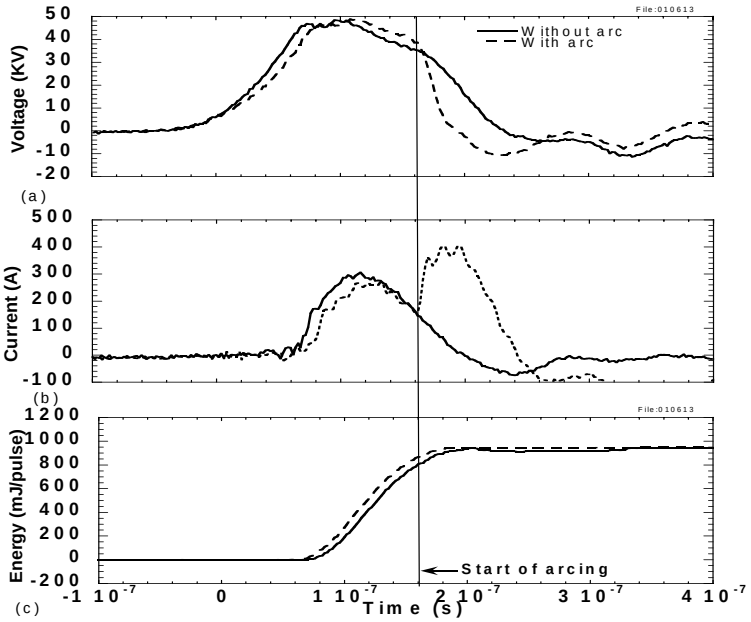

Figure 19.Voltage (a), Current (b) and Energy (c) of pulsed corona discharge with (dash curve) and without (solid curve) arc. Energy: 956mJ/pulse. Tests performed in cylindrical test chamber

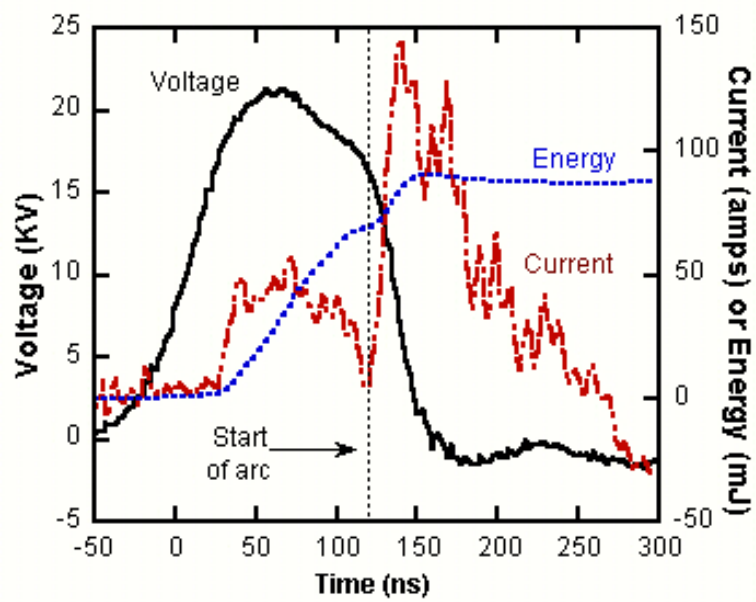

Figure 20. Plot of Voltage, Energy and Current delivered to the gas for Corona discharge plus Arc. Test performed in engine cylinder test chamber.

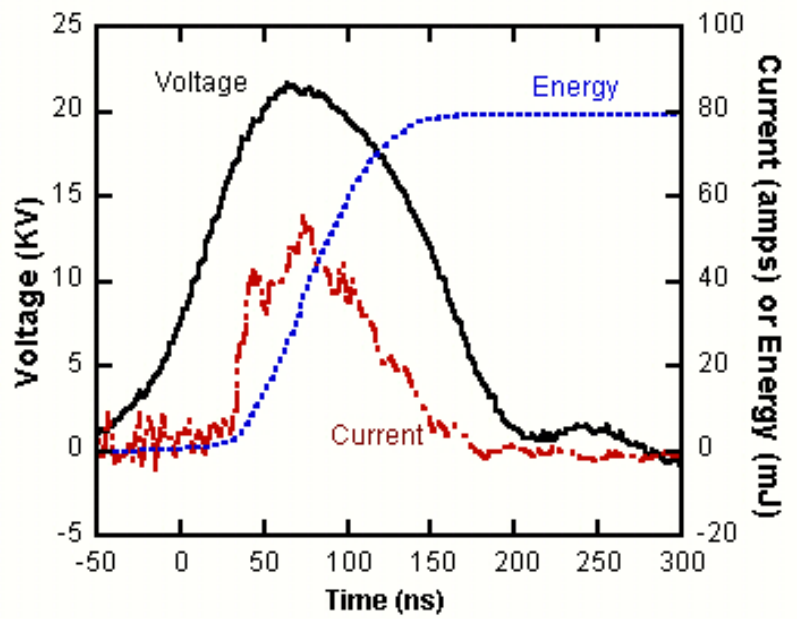

Figure 21. Plot of Voltage, Energy and Current delivered to the gas for Corona discharge only. Test performed in engine cylinder test chamber.

B. Combustion Characteristics

Figure 22 shows a typical pressure waveform. The pressure rose slowly after trigger for a period of time, then suddenly increased rapidly at a certain point, reached its maximum and finally dropped gradually. We define ignition delay time as the interval between trigger and the moment at which the pressure rises to 10% of its maximum value. Pressure rise time is defined as the interval between moments at which pressure rises to 10% and 90% of its maximum value. Peak pressure is the maximum pressure during entire process.

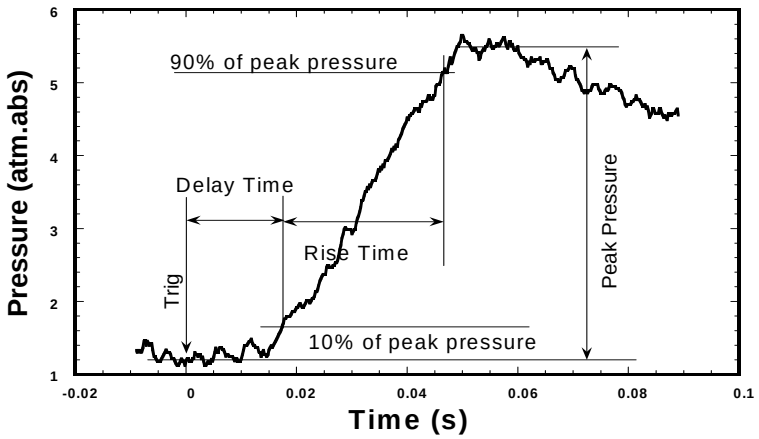

Figure 22. Typical pressure waveform with definitions of ignition delay time, pressure rise time and peak pressure.

Figure 23 shows the pressure rise time as a function of corona pulse energy for various equivalence ratios. For each equivalence ratio there is an energy value (e.g. ~300mJ/pulse for equivalence ratio 1.0), below which the pressure rise time decreases rapidly as pulse energy increases, and above which the pressure rise time is approximately constant. This behavior shows that pulsed corona discharge does affect flame ignition, and there is an "optimal energy", pulse energy higher than optimal energy is not necessary for ignition improvement. This optimal energy increases as equivalence ratio decreases. Similar tendencies are found in curves of ignition delay time (Fig. 24) and peak pressure versus corona pulse energy. When the pulse energy is smaller than optimal energy, ignition delay time decreases and peak pressure increases as pulse energy increases. When pulse energy is larger than optimal energy, all these parameters are approximately constant as pulse energy varies.

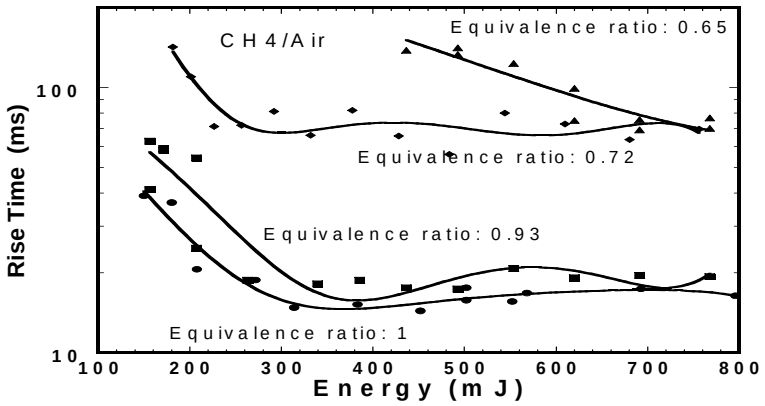

Figure 23. Pressure rise time versus pulse energy for various equivalence ratios.

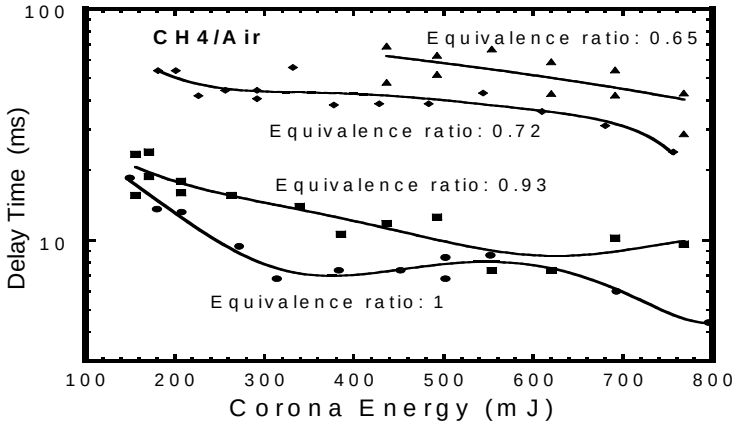

Figure 24. Ignition delay time versus pulse energy for various equivalence ratios.

Three different electrode geometries were tested in the engine cylinder test chamber, a ring shaped electrode, a straight electrode and a single pin point electrode. The ring electrode allowed the most electrical energy to be deposited to the gas before arcing so it was used for the corona combustion tests. Due to the smaller chamber size of the engine cylinder test chamber the center electrode is much closer to the chamber walls than in the larger cylindrical test chamber and is more likely to arc. Arcing usually occurs at the tip

of the electrode or at a sharp bend. In order to prevent the electrode from arcing the end of the electrode was insulated. Without this insulation the energy of the corona was too low to ignite the air/fuel mixture in the cylinder. Figure 25 shows the pressure rise time in the engine cylinder test chamber for corona only ignition, corona plus arc and for a conventional spark plug. It can be seen that the corona ignition delivers a steeper pressure rise than the conventional spark plug and a higher peak pressure. When the power was increased to allow the corona to arc the peak pressure was higher than the corona alone but it comes at the expense of additional electrical energy needed to produce the arc.

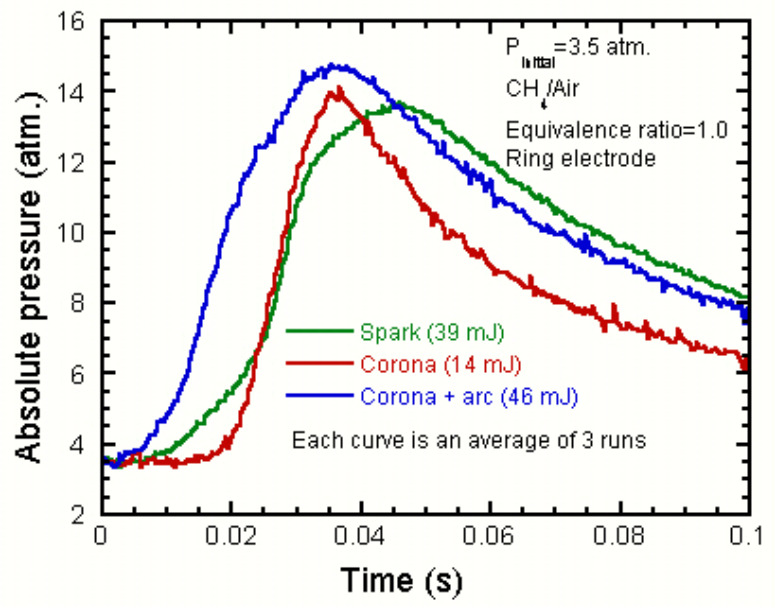

Figure 25. Plot of Pressure vs. Time for Corona, Corona + arc and conventional spark plug with associated electrical energy. Tests performed in engine cylinder test chamber.

Figures 26-28 show the dependence of ignition delay time, pressure rise time and peak pressure on equivalence ratio for iso-octane/air mixtures ignited by pulsed corona discharge as well as by spark discharge at pressures of 1.0 and 0.6 atm. Since the combustion properties of flame ignited by spark discharges are dependent on the location of the igniter, different locations of spark plug were tested and the optimum location is at center of the test cylinder. In the text below, whenever comparison is made between pulsed corona and spark discharge ignition with spark ignition at the center of the test cylinder.

As shown in Figs. 26-28, in the equivalence ratio range of 0.8 to 1.4 and initial pressure of 0.6 and 1.0 atm., C_8H_{18}/Air flames ignited by pulsed corona discharge have similar tendencies to flames ignited by spark discharges, but shorter ignition delay time, shorter (by a factor of 2) pressure rise time and higher peak pressure than spark-ignited discharges. Experiments with methane, propane, isobutene, n-butane and iso-octane show similar behavior.

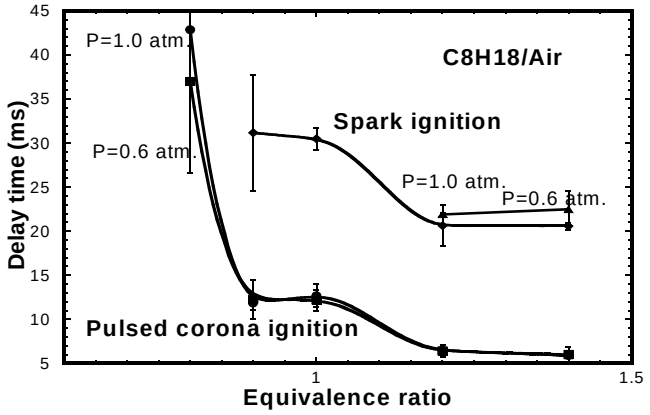

Figure 26. Ignition delay time versus equivalence ratio of C_8H_{18}/Air flames: Comparison between pulsed corona and spark ignition. Corona discharge energy: 1521mJ (1 atm.) 1509mJ (0.6atm.). Spark Energy: 70mJ (1 atm.) 68mJ (0.6 atm.).

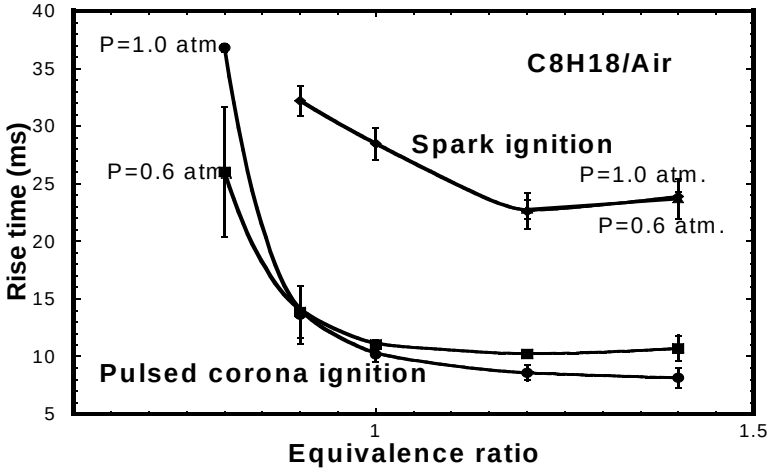

Figure 27. Pressure rise times versus equivalence ratio of C_8H_{18}/Air flame. Comparison between pulsed corona and spark discharge ignition. Energy same as Fig. 18.

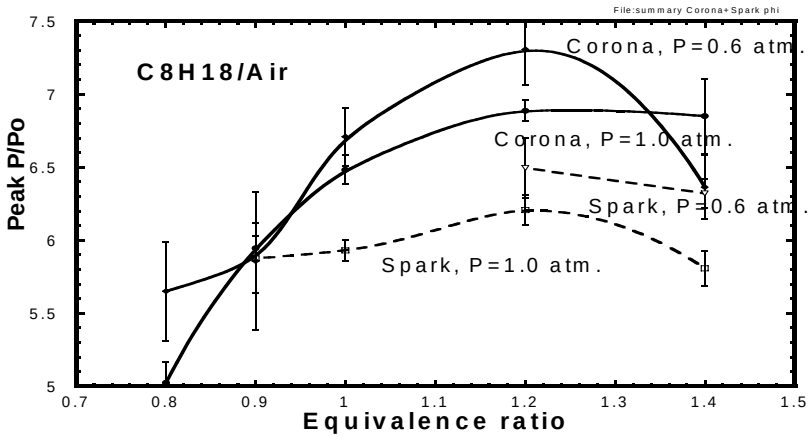

Figure 28. Peak pressure versus equivalence ratio of C_8H_{18}/Air flame. Comparison between corona and spark ignition. Energy same as Fig. 26.

Testing was done in the cylindrical chamber with the turbulence generator to explore the effects of turbulence on the performance of corona ignition. Spark data was also collected under turbulent conditions for comparison (Fig. 29.). It was found that turbulent cases have faster rise times, higher peak pressures and faster decay than the quiescent cases (due to heat losses in the burned gas). The delay times were not affected by turbulence for both corona and spark ignitions, thus transport does not play a large role in delay time.

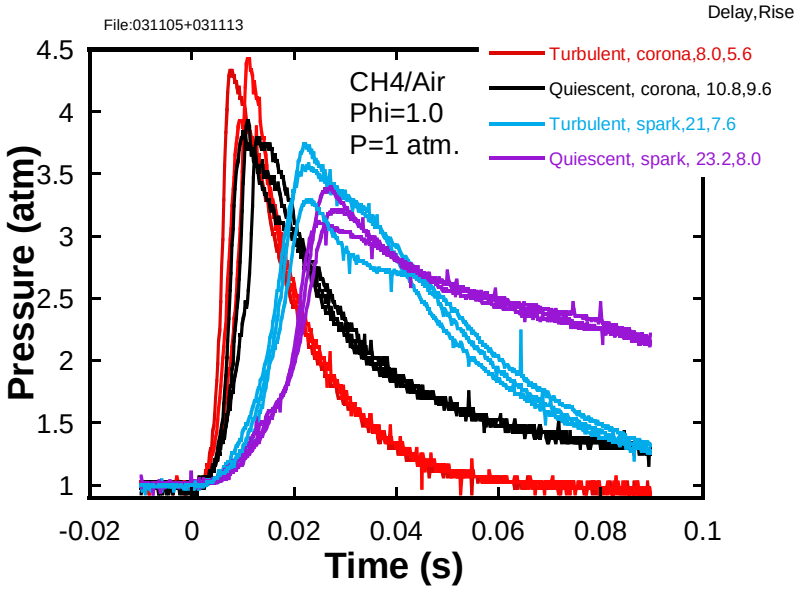

Figure 29. Pressure vs. Time plots for turbulent and quiescent cases for both corona and spark plug ignition.

C. Initial On-Engine Testing

The corona was run as the ignition source on one cylinder of the test engine for a short duration test. Some problems were encountered with the engine tests that must be solved before testing can continue. One major issue is that the corona discharge is immediately followed by an arc due to the close proximity of the electrode to the cylinder head (approx ¼"). In bench tests this problem was easily solved by using silicone rubber or ceramic paste. Obviously these methods won't work inside a running engine so alternative coatings must be found and are being explored. The capacitor on the corona generator is discharged much faster when the electrode is arcing and cannot recharge fast enough to run continuously at engine speeds. This will be less of a problem once insulation is in place to prevent arcing as the arcing drains the capacitors much more quickly than the corona discharge by itself. Another issue that must be addressed is the EMF noise emitted from the corona generator and high voltage lead. This caused some problems with the engine control system and damaged one of the data acquisition cards. Proper shielding and grounding should resolve this issue. Despite these problems encountered while running with the corona, a noticeable increase in cylinder pressure was seen when the corona was enabled as seen in Figure 30.

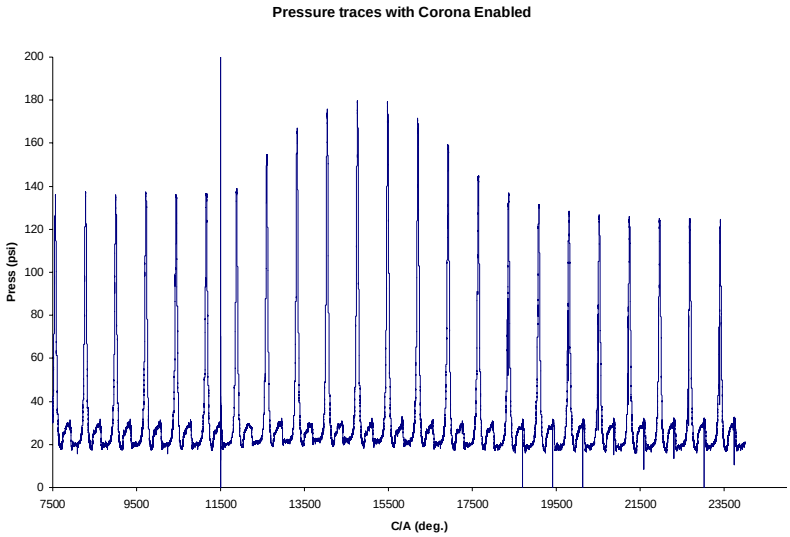

Figure 30. Plot of cylinder pressure traces as a function of C/A. Higher pressures occurred when the Corona is enabled.

During the short on-engine testing cylinder pressure was logged and the pressure trace is shown below in Fig 31. The engine speed audibly increased when the corona was enabled.

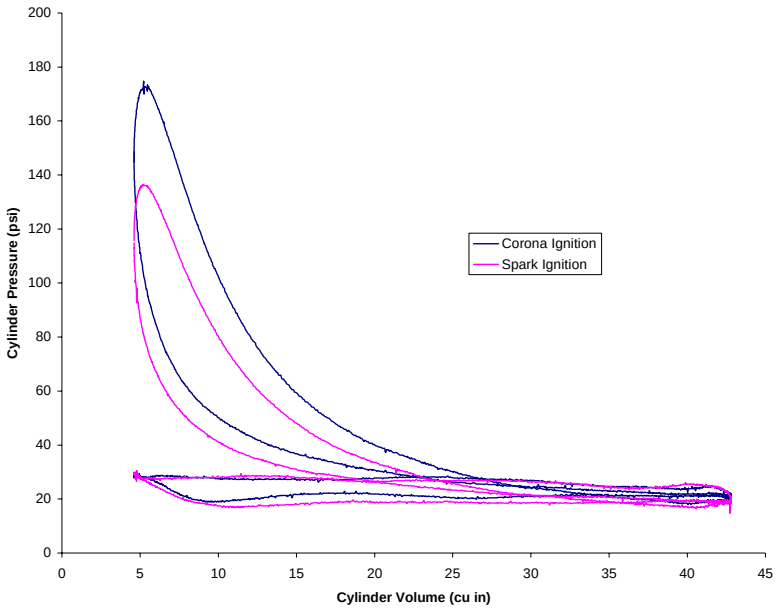

Figure 31. PV diagram showing increase in IMEP with Corona enabled.

Various coatings are currently being tested to determine what will insulate against the high voltage corona discharge and hold up under the harsh conditions inside the combustion chamber. Aluminum oxide looks promising as it has a very high dielectric strength (up to 1000 V/mil) and can be plasma sprayed onto engine components providing a good bond.

Conclusion

An advantage of the pulsed corona discharge ignition occurs as the result of the creation of several hundred spatially distributed discharges. This is produced by the transient high field condition, and cannot occur for an extended time, thus is a result of the different characteristics (the complex electron energy distribution and concomitant collisional electron excitation processes). This fills a large portion of the test cylinder as compared to the single discharge channel for conventional spark discharges. Depending on how many discharge channels have enough energy to ignite flames, this multi-site ignition mechanism significantly reduces the times necessary for chemical reaction propagation, resulting shorter ignition delay and pressure rise times. Chemical advantages of corona discharges are related to the higher initial concentration of radicals created by the higher electron energy of the pulsed corona process. Computations [20, 21] show that radical ignition sources exhibit about half the ignition delay (defined as time difference between energy deposition and virtual time origin of the steadily propagating flame) of thermal ignition sources having the same energy input (though minimum ignition energies are similar for radical and thermal sources).

Initial on-engine testing looks promising and has already shown improved combustion over the standard spark plug ignition. Higher peak pressures, faster rise times and a higher IMEP were all realized with the corona discharge ignition. Once the issues of EMF, piston and head insulation, and capacitor recharge time are addressed, engine testing will resume. The EMF issue can be solved by properly shielding the generator, using a shielded coaxial wire for the high voltage lead, and isolating the control system and corona generator grounds. Finding an adequate ceramic coating to insulate a portion of the piston surface and cylinder head will prevent the arcing that is occurring during on-engine tests and will keep from discharging the capacitors so rapidly allowing for longer duration tests. The issue with electrically insulating the piston an cylinder head is not expected to be an issue when running on large stationary natural gas engines. This is due to the larger gap that can be achieved between the corona electrode and piston / cylinder head in a large stationary engine. Experimentally it was found that if the spacing between the electrode and ground surface (i.e. piston and cylinder head) is on the order of 25 mm (~1 inch) or more that insulation is not necessary. Therefore once the shielding issue is solved a stationary engine test could be conducted.

References

[1] J.B.Heywood. Internal combustion engine fundamentals, McGraw-Hill, New York, 1988.

[2]. J. D. Dale, P. R. Smy, and R. M. Clements, "Laser Ignited Internal Combustion Engine - An Experimental Study," *SAE Paper No. 780329* (1978.)

[3] Kailasanath, K., "Review of propulsion applications of detonation waves," *AIAA J.*, Vol. 38, pp. 1698-1708 (2000); Kailasanath, K., "A review of PDE research - performance estimates," AIAA Paper 2001-0474 (2001).

[4] Schauer, F., Stutrud, J., Bradley, R., "Detonation initiation studies and performance results from pulsed detonation engine applications," AIAA Paper No. 2001-1129 (2001).

[5] Bussing, T. R. A., Bratkovich, T. E., and Hinkey, J. B., "Practical Implementation of Pulse Detonation Engines," AIAA Paper 97-2748, July 1997.

[6] Cote, T., Ridley, J.D. Clements, R.M. Smy, P.R., "The ignition characteristics of igniters at sub-atmospheric pressure", Combust. Sci. and Tech. Vol.48, pp 151-162, 1986.

[7] D. Yossefi, S.J. Maskell, S.J. Ashcroft and M.R. Belmont,"Ignition source characteristics for naturel-gas-buring vehicle engines", Proc Instn. Mech Engrs Vol 214 Part D 171-180,2000

[8] M. Lavid, A.T. poulos, S.K. Gulati, Y. Nachshon and J.G. Stevens, "Excimer laser relight for the supersonic commercial transport aircraft" SPIE Vol. 1862 , 59-70 (1993)

[9] R. Maly, "Spark ignition: Its physics and effect on the internal combustion engine" in "Fuel Economy in road vehicles powered by spark ignition engines" ed. J.C. Hilliard and G.S.Springer, Plenum Press, New York , 1984, 91-148

[10] R. Maly and M. Vogel, "Initiation and propagation of flame fronts in lean CH4-air mixtures by the three modes of the ignition spark" Seventeenth Symposium (International) on Combustion 821-831, The Combustion Institute, 1978

[11] R. Maly," Ignition model for spark discharge and the early phase of flame front growth" Eighteenth Symposium (International) on Combustion 1747-1753, The Combustion Institute, 1981

[12] E.M. Bazelyan and Yu.P. Raizer, "Spark Discharge", CRC Press, Boca Raton, New York, 1998.

[13] Y.L.M. Creyghton, "Pulsed positive corona discharges", Thesis Eindhoven, 1994.

[14] Roth, G.J., and Gundersen, M.A., "Laser induced fluorescence of NO distribution after needle-plane pulsed negative corona discharge, IEEE transactions on plasma science, Vol. 27,No. 1 28-29

[15] Puchkarev, V., Roth, G., and Gundersen, M, "Plasma processing of diesel exhaust by pulsed corona discharge", International fall fuels and lubricants meeting and exposition, San Francisco, California, Oct. 19-22,1998, SAE technical paper series 982516

[16] These results have been reported at AFOSR and ONR contractors meetings. Additional details are provided at: http://carambola.usc.edu.

[17] Civitano, L., "Industral application of pulsed corona processing to flue gas",in " Non-Thermal plasma techniques for pollution control" ed. Penetrante, B.M. and Schultheis, S.E., Springer-Verlag Berlin Heidelbers, 1993, 0.3-130.

[18] M. Goldman and A. Goldman, "Corona discharge" in "Gaseous Electronics" ed. M.N. Hirsh and H.I. Oskam, 219-291.

[19]Y.L.M. Creyghton. E.M. van Veldhuizen and W.R. Rutgers, Electrical and optical study of pulsed positive corona, in Non-Thermal Plasma Techniques for pollution control edited by B.M. Penetrante and S. Schultheis, Springer-Verlag Berlin Heidelberg, 1993

[20]. Dixon-Lewis, G., Shepard, I.G., *Proc. Combust. Inst.* 15:1483-1491 (1974).

[21]. T. M. Sloane, *Combust. Sci. Tech.* 73:351-365, 1990.

[22]. Lewis, B., von Elbe, G., *Combustion, Flames, and Explosions of Gases*, 3rd Ed., Academic Press, 1987.

[23] JianBang Liu, Paul D. Ronney, Fei Wang, L.C. Lee and Martin Gundersen, "Transient plasma ignition for lean burn applications" 41st Aerospace Sciences Meeting, 5th Weakly Ionized Gases Workshop, Reno, Nevada 6 - 9 Jan 2003

[24] Martin A. Gundersen, Andras Kuthi and Jianbang Liu, "Transient plasma ignition physics for pulse detonation engines" 15th ONR propulsion meeting, Washington, DC, August 5-7, 2002